



# Automatic Removal of Fringes from EFOSC Images

Colin Snodgrass, Benoît Carry

## ► To cite this version:

Colin Snodgrass, Benoît Carry. Automatic Removal of Fringes from EFOSC Images. The Messenger, 2013, 152, pp. 14-16. hal-00844047

**HAL Id: hal-00844047**

**<https://hal.science/hal-00844047>**

Submitted on 12 Jul 2013

**HAL** is a multi-disciplinary open access archive for the deposit and dissemination of scientific research documents, whether they are published or not. The documents may come from teaching and research institutions in France or abroad, or from public or private research centers.

L'archive ouverte pluridisciplinaire **HAL**, est destinée au dépôt et à la diffusion de documents scientifiques de niveau recherche, publiés ou non, émanant des établissements d'enseignement et de recherche français ou étrangers, des laboratoires publics ou privés.

# Automatic Removal of Fringes from EFOSC Images

Colin Snodgrass<sup>1</sup>Benoît Carry<sup>2</sup><sup>1</sup> Max Planck Institute for Solar System Research, Katlenburg-Lindau, Germany<sup>2</sup> Institut de Mécanique Céleste et de Calcul des Éphémérides (IMCCE), Observatoire de Paris, France

EFOSC, in common with many instruments with older CCDs, shows a fringe pattern in images taken at red wavelengths. These fringes are difficult to remove without significant manual adjustment for each individual frame, which is a time-consuming exercise, but necessary for reliable photometry of faint objects across the whole field of view. We present a simple technique to automatically remove fringes from CCD images, and provide scripts (available on the ESO website) to apply this to EFOSC data, or to any other images.

## Fringing in CCD images

Astronomical charge-coupled device (CCD) images are often affected by fringe patterns (Figure 1a). These fringes are created by the interference of monochromatic light within the CCD. Narrowband filters are typically affected, as well as broadband filters containing strong sky emission lines. Lines due to atmospheric OH affect bandpasses at the red end of the CCD wavelength range ( $\lambda > 700$  nm), i.e., *R*-, *I*- and *Z*-bands. The problem is discussed in more detail in the broad introductions to CCD data reduction by Gullixson (1992) and Howell (2006), and in the recent paper by Howell (2012). While the latest generation of CCDs does not suffer from this problem, there are many instruments still in active use (such as EFOSC2 at the New Technology Telescope [NTT]; Buzzoni et al., 1984) that employ older CCDs. Given the increasing popularity of ESO's archival data in publications, removal of fringes from images remains a necessary reduction step for many users.

Fringes are a cosmetic problem — obvious to the human eye when a typical “z-scale” algorithm is used to display astronomical images — but add only a

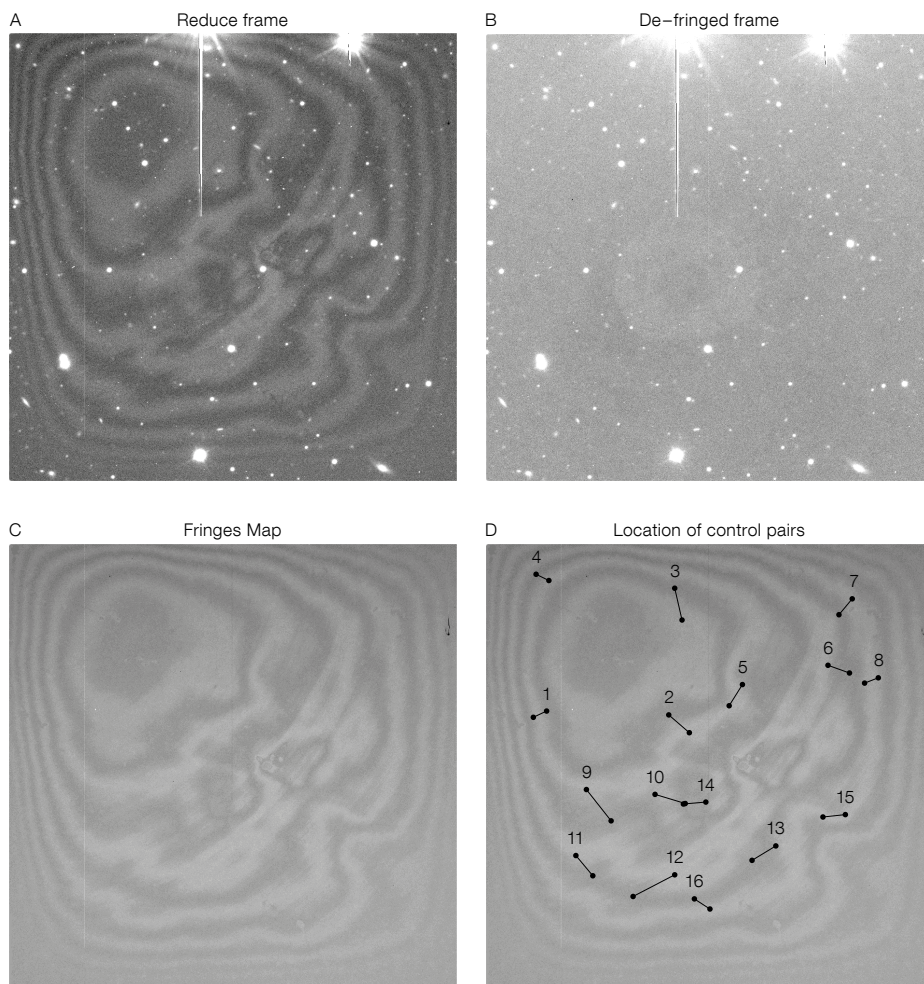


Figure 1. a) *R*-band EFOSC2 frame presenting a strong fringe pattern (following standard reduction steps: bias subtraction and flat fielding); b) same as a), but after application of the defringing method presented here; c) the fringe map used in the correction; d) location of the control pairs used to scale the fringe map (see text).

small additional flux to the image. For shorter exposure images they are hardly noticeable and attempts to remove them can be more trouble than they are worth (even a good fringe map has some associated noise, and it is worth remembering that all reduction steps add noise to the image; Newberry [1991]). However, for longer exposures, and especially when dealing with photometry of multiple or extended objects, or of moving targets, it can be critical to remove the fringes to provide properly uniform photometry across the field. As calibrations (biases, flats) are taken during the day, or during twilight, they do not show the faint night

sky-emission fringes and cannot be used for correcting the fringe patterns. Therefore, fringes are not removed by the standard data-processing techniques (bias subtraction, bad pixel masking, and flat-fielding). Fringe removal requires an extra step, where a description of the fringe pattern is scaled and subtracted from each image. This has traditionally been a rather labour-intensive step, typically requiring careful manual adjustments for each science image, as the intensity of the fringes is highly variable, depending on atmospheric conditions.

## Properties of the fringes

The location of the fringes in the images is determined by changes in the thickness of the CCD. Hence, the pattern of the fringes on the detector is globally stable with time. The intensity of the fringes

depends on the amount of incoming monochromatic light, either from the sky emission lines or selected by a narrow-band filter. The fringes can therefore present large intensity variations from image to image, even during a single night of observation, reaching up to several percent of the noise level from the sky background. This variability presents the largest challenge in correcting for fringing, as care has to be taken to scale the fringe pattern to the correct intensity for each image individually before subtraction.

The stability of the fringe pattern means that a single high signal-to-noise (S/N) fringe map can be used to describe the pattern. These are generally created through a combination of frames taken of the night sky (under moonless conditions, as a bright sky background can mask the faint fringes). When data are taken of a given target with a significant jitter pattern — i.e., movement of the telescope in a random fashion between each image, so that sources do not fall on the same pixels in multiple images — then the data frames themselves can be median-combined to leave only the fringe pattern. Alternatively, images of a deliberately selected “empty” field can be used, but this uses a significant amount of good observing time for calibration. Howell (2012) describes a new method of constructing a fringe map using neon lamp illumination during daytime calibrations, which has the advantage that very high S/N can be achieved without wasting any time during the night. For EFOSC, a pre-prepared fringe map is available for download<sup>1</sup>. Fringe maps for EFOSC have been measured through different filters and at different times (including before and after moving the instrument from the 3.6-metre telescope to the NTT — see Snodgrass et al. [2008]), and demonstrate the stability of the fringe pattern and the fact that it is almost identical in different passbands.

Once a fringe map is obtained by any of the above methods it has to be scaled to the intensity of the fringe pattern in each science frame, and then subtracted from the data. Note that the fringe pattern is additional flux, so it is subtracted from the data, unlike flat-field variations, which are corrected by division. Here lies the difficulty in the operation, as the intensity

of the fringe pattern is highly variable on short timescales. In general it increases with increasing exposure time (longer exposures are more significantly affected), so to first order the pattern can be scaled by the length of each exposure. This is the approach used by the fringe removal option within the widely used *ccdproc* task in IRAF (part of the core *ccdred* package; Valdes [1988]), but this method can considerably over- or under-correct due to the intrinsic variations of the night sky-emission lines, which are not correlated to exposure time. The *ccdproc* task also gives the option of specifying additional scaling factors via image headers, but this requires considerable manual iteration to get a satisfactory result. It is worth noting that the same IRAF package also includes the *mkfringecor* task, which is used to combine frames to construct a good fringe map.

A second approach implemented within IRAF is to scale the fringe map to globally minimise the difference between the map and object frames, which is used by the *rmfringe* and *irmfringe* tasks in the *mscared* package (Valdes, 1998). This approach works better, but requires careful masking of sources, bad pixels and cosmic rays to avoid these affecting the minimisation. It therefore needs some preparatory work, and can be time consuming when dealing with many frames (especially where these are of different fields).

### Automatic de-fringing method

Here we describe a method that allows frames to be processed simply and automatically, with minimal preparation beyond the construction of the fringe map. We take advantage of the stability of the shape of the fringe pattern to clean it from the scientific frames, by using knowledge of the pattern to define areas of each image to perform automatic scaling. We describe the fringe pattern in terms of “dark” and “bright” areas, corresponding to the background sky and the fringes themselves (see Figure 1c). The precise choice of areas is not important, providing they sample the variation in the fringe pattern well (in practice, any sufficiently large number of random points will work).

To estimate the amplitude of the fringe pattern, we measure the flux difference between bright and dark areas. Practically, we use a series of “control pairs”, each consisting of a couple of reference locations, taken in and out of the fringe pattern (Figure 1d). For each pair  $i$ , we measure the flux difference on the frame between the bright and dark area,  $\delta F_i = F_{\text{bright}} - F_{\text{dark}}$ , and, at the same position on the fringe map, the flux difference between the bright and dark areas,  $\delta M_i$ . The scale factor to be applied to the fringe map is then taken as the median of all the ratios,  $\delta F_i / \delta M_i$ . Theoretically, a single control pair would be enough to scale the fringe map. However, the presence of any astronomical source (star, galaxy, nebula, etc.) close to one of the ends of the control pair would bias the scale factor. Therefore we select several control pairs (typically 5 to 20) spread across the full field. Experimentation with the number and position of the pairs has shown that the quality of the subtraction is hardly affected by these factors.

The list of control pairs is based on the constant fringe pattern, so it can be fixed for a given instrument, and does not need to be modified for different data-sets — with a sufficient number of pairs the occasional overlap of a pair with a source doesn’t affect the scaling. This allows highly automated de-fringing — once a fringe map and a suitable set of pairs are defined for a given instrument, the de-fringing operation does not require further human intervention. As the measurement of each pair is a simple operation, a large number can be used without any concerns about computing time. The scripting of this operation is relatively straightforward — we provide implementations in two popular systems used for astronomical data reduction, IDL and IRAF. A table of control points for EFOSC is provided with the code<sup>1</sup>.

The same approach has been applied as part of the Elixir pipeline for data from the MegaCam instrument at the Canada-France-Hawaii Telescope (Magnier & Cuillandre, 2004; Regnault et al., 2009). The scripts we provide implement a more general solution, designed to work with EFOSC, but applicable to all imaging data with no modification.



### Example: photometry of trans-Neptunian objects

As an example of the method presented here, we present an image taken from a photometric survey of faint trans-Neptunian objects; members of a dynamical family related to the dwarf planet (136108) Haumea (Snodgrass et al., 2010; Carry et al., 2012). We measured visible colours (in *BVRi*-bands) and rotational light curves (*R*-band) of 30 targets with *V* magnitudes between approximately 20 and 24, using EFOSC. All the targets were moving relative to the comparison field stars, alternatively coming in and out of the fringe pattern (Figure 1a), and were therefore affected by it at a level that could have a significant influence on the photometry, especially for the faintest targets. We removed the fringe pattern using the method described here, and present the cleaned version of an example frame in Figure 1b. In this particular example, a faint circle is visible near the centre of

the image, which is not part of the fringe pattern but a ghost reflection due to the bright star just off of the top of the frame. Such a faint structure is nearly impossible to identify in the original frame due to the fringes. Jitter patterns were employed to allow new fringe frames to be created, and with many moving targets observed over three multi-night runs, a large number of different fields were observed, including some relatively dense star fields. All were automatically processed via this method with no manual adjustments required. Our method has also been successfully applied to EFOSC images of extended sources (active comets) by Lacerda (2013).

### References

- Buzzoni, B. et al. 1984, *The Messenger*, 38, 9  
 Carry, B. et al. 2012, *A&A*, 544, A137  
 Gullixson, C. A. 1992, in *ASP Conference Series*, Vol. 23, *Astronomical CCD Observing and Reduction Techniques*, ed. S. B. Howell, 130

- Howell, S. B. 2006, *Cambridge observing handbooks for research astronomers*, Vol. 5, *Handbook of CCD Astronomy*, eds. R. Ellis, J. Huchra, S. Kahn, G. Rieke & P. B. Stetson, (Cambridge: Cambridge University Press)  
 Howell, S. B. 2012, *PASP*, 124, 263  
 Lacerda, P. 2013, *MNRAS*, 428, 1818  
 Magnier, E. A. & Cuillandre, J.-C. 2004, *PASP*, 116, 449  
 Newberry, M. V. 1991, *PASP*, 103, 122  
 Regnault, N. et al. 2009, *A&A*, 506, 999  
 Snodgrass, C. et al. 2010, *A&A*, 511, A72  
 Snodgrass, C. et al. 2008, *The Messenger*, 132, 18  
 Valdes, F. 1988, in *Instrumentation for Ground-Based Optical Astronomy*, ed. L. B. Robinson, 417  
 Valdes, F. G. 1998, in *ASP Conference Series*, Vol. 145, *Astronomical Data Analysis Software and Systems VII*, eds. R. Albrecht, R. N. Hook, & H. A. Bushouse, 53

### Links

- <sup>1</sup> Pre-prepared EFOSC fringe image and de-fringing scripts from: <http://www.eso.org/sci/facilities/lasilla/instruments/efosc/inst/fringing.html>



Colour-composite image of the large planetary nebula IC 5148 taken with EFOSC2 on the New Technology Telescope at La Silla (image size 4.2 by 4.2 arcminutes) formed from exposures in *B*, *H $\beta$* , *V*, *R* and *H $\alpha$*  filters. The nebula morphology consists of two distinct shells but the bright ansae indicate more complex substructure. The emission nebula is of high ionisation and the very hot central star is obvious. See Picture of the Week 15 October 2012 for more information.